Disrupted cardiac development but normal hematopoiesis in mice deficient in the second CXCL12/SDF-1 receptor, CXCR7

Frederic Sierro*, Christine Biben†, Laura Martínez-Muñoz‡, Mario Mellado‡, Richard M. Ransohoff§, Meizhang Li§, Blanche Woehl*, Helen Leung*, Joanna Groom*, Marcel Batten*¶, Richard P. Harvey†, Carlos Martínez-A‡, Charles R. Mackay*, and Fabienne Mackay*‖

*Department of Immunology and Inflammation, Garvan Institute of Medical Research, 384 Victoria Street, Darlinghurst NSW 2010, Australia; †Victor Chang Cardiac Research Institute, 384 Victoria Street, Darlinghurst NSW 2010, Australia; ‡Department of Immunology and Oncology, Centro Nacional de Biotecnología/CSIC, Campus de Cantoblanco, E-28049 Madrid, Spain; and §Neuroinflammation Research Center, Department of Neurosciences, Lerner Research Institute, Cleveland Clinic Foundation, 9500 Euclid Avenue, Cleveland, OH 44195

Edited by Dan R. Littman, New York University Medical Center, New York, NY, and approved July 27, 2007 (received for review March 10, 2007)

Chemotactic cytokines (chemokines) attract immune cells, although their original evolutionary role may relate more closely with embryonic development. We noted differential expression of the chemokine receptor CXCR7 (RDC-1) on marginal zone B cells, a cell type associated with autoimmune diseases. We generated *Cxcr7*$^{-/-}$ mice but found that CXCR7 deficiency had little effect on B cell composition. However, most *Cxcr7*$^{-/-}$ mice died at birth with ventricular septal defects and semilunar heart valve malformation. Conditional deletion of *Cxcr7* in endothelium, using *Tie2-Cre* transgenic mice, recapitulated this phenotype. Gene profiling of *Cxcr7*$^{-/-}$ heart valve leaflets revealed a defect in the expression of factors essential for valve formation, vessel protection, or endothelial cell growth and survival. We confirmed that the principal chemokine ligand for CXCR7 was CXCL12/SDF-1, which also binds CXCR4. CXCL12 did not induce signaling through CXCR7; however, CXCR7 formed functional heterodimers with CXCR4 and enhanced CXCL12-induced signaling. Our results reveal a specialized role for CXCR7 in endothelial biology and valve development and highlight the distinct developmental role of evolutionary conserved chemokine receptors such as CXCR7 and CXCR4.

chemokines | heart | heterodimerization | immunology | endothelium

Chemokines are chemoattractant cytokines that bind to G protein-coupled seven-transmembrane receptors (GPCRs). They facilitate leukocyte migration but can also play a role in embryogenesis and angiogenesis (1, 2). CXCL12 (SDF-1) and its receptor CXCR4 are essential for heart, CNS, and blood vessel development, as well as B cell lymphopoiesis (3–7). Targeted deletion of *Cxcl12* or *Cxcr4* in the mouse leads to similar phenotypes, including ventricular septal defects, disorganized cerebellum, impaired hematopoiesis, and embryonic lethality between embryonic day (E)15 and E18 of gestation. Thus, CXCL12 and CXCR4 were long thought to be a monogamous pair. However, recent studies show that CXCL12 binds to an additional chemokine receptor, CXCR7 (RDC1/Cmkor1) (8, 9). In addition to CXCL12, CXCR7 binds to the chemokine CXCL11, although with a lower affinity (9). *Cxcr7* encodes a protein highly conserved in mammals with >91% identity and 95% similarity between human, mouse, and dog proteins. It was first identified as an orphan GPCR expressed in the human thyroid and related to the chemokine receptor CXCR2 (10). Both CXCR7 and CXCR4 are expressed in a wide range of tissues in humans and are up-regulated in some tumors (9, 11–13). Similar to CXCR4, CXCR7 can facilitate angiogenesis (9, 14), and blockade of CXCR7 (9) or CXCR4 (12) inhibits tumor growth in several mouse models.

Cxcr7 gene conservation throughout evolution and the affinity of CXCR7 for CXCL12 suggest that *Cxcr7* may also play a role in lymphopoiesis or embryogenesis. The present study reports on the characterization of *Cxcr7*$^{-/-}$ mice or mice conditionally deficient for *Cxcr7* in the endothelium. We show that *Cxcr7* is a gene essential for heart valve formation but appears to play no obvious role in hematopoietic or nervous system development. This nonsignaling receptor may mediate some of its effects through heterodimerization with CXCR4, although the significance of this effect *in vivo* remains unclear.

Results

CXCR7 Is Expressed on a Subset of Mouse and Human B Lymphocytes. We examined the expression of *Cxcr7* using public databases (http://symatlas.gnf.org/SymAtlas) (15) and found that in humans, *CXCR7* was expressed in a wide range of tissues. Using a large data set of Affymetrix Genechip expression analyses of human immune cells (16, 17), we found that, within the immune system, *Cxcr7* transcripts were present in only a restricted subset of leukocytes, some T cell subsets, and NK cells, as well as in B cells (Fig. 1*A*). *Cxcr7* transcripts were mostly expressed in B cells (Fig. 1 *A–C*) at high levels, particularly in the human memory B cell subset (Fig. 1*B*), as reported (18), in mouse splenic marginal zone (MZ) B cells and in transitional type 2 MZ precursors (Fig. 1*C*). This expression pattern was different from that of the other CXCL12 receptor, CXCR4, suggesting distinct roles in the immune system.

Normal Hematopoiesis, CNS, and Gastrointestinal Vasculature in *Cxcr7*$^{-/-}$ Mice and Modest Reduction in MZ B Cell Numbers. To dissect the role of *Cxcr7* in development and/or immune responses, we generated *Cxcr7*-deficient mice using a conditional approach [supporting information (SI) Fig. 6 *A–C*] and noted rapid postnatal death of >95% of *Cxcr7*$^{-/-}$ neonates within 24 h (SI Fig. 6*D*). Development of B cells and granulocytes in fetal liver and bone marrow was normal (Fig. 1*D* and SI Fig. 7), in contrast

Author contributions: F.S. and C.B. contributed equally to this work; F.S., C.B., M.M., C.M.-A., C.R.M., and F.M. designed research; F.S., C.B., L.M.-M., M.L., B.W., H.L., J.G., and M.B. performed research; F.S., C.B., L.M.-M., R.M.R., and M.L. analyzed data; and F.S., C.B., M.M., R.P.H., C.M.-A., C.R.M., and F.M. wrote the paper.

The authors declare no conflict of interest.

This article is a PNAS Direct Submission.

Abbreviations: SLV, semilunar valve; ISH, *in situ* hybridization; E*n*, embryonic day *n*; MZ, marginal zone; CFP, cyan fluorescent protein; YFP, yellow fluorescent protein.

Data deposition: The data reported in this paper have been deposited in the Gene Expression Omnibus (GEO) database, www.ncbi.nlm.nih.gov/geo (accession no. GSE8710).

¶Present address: Department of Molecular Biology, Genentech, South San Francisco, CA 94080.

‖To whom correspondence should be addressed. E-mail: f.mackay@garvan.org.au.

This article contains supporting information online at www.pnas.org/cgi/content/full/0702229104/DC1.

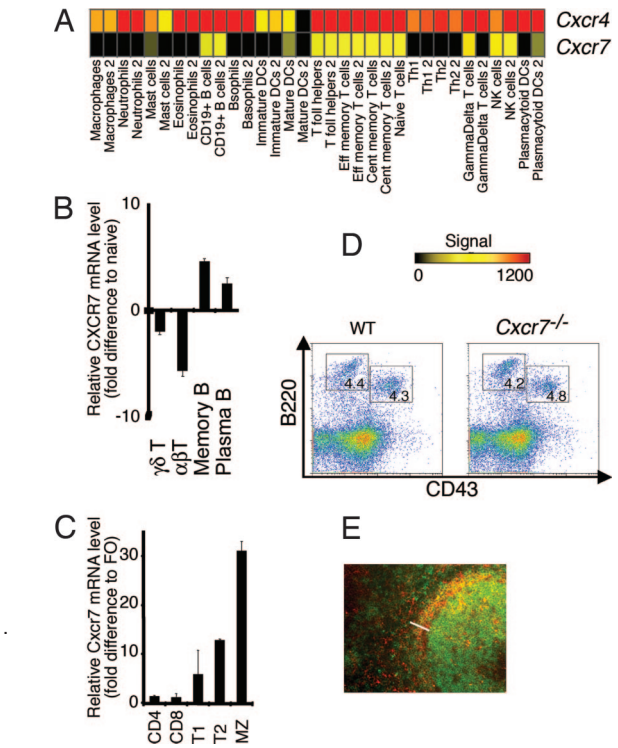

Fig. 1. *Cxcr7*$^{-/-}$ mice develop a normal immune system. (*A*) *CXCR7* and *CXCR4* expression patterns in human resting leukocyte subsets. The color scale indicates transcript signal where black = absent, yellow = moderately expressed, and red = highly expressed. *Cxcr7* mRNA levels quantitated by real-time PCR in human (*B*) and murine (*C*) T and B cells relative to naive or follicular (FO) B cells, respectively. Values ± SEM. (*D*) E17.5 fetal liver cells were stained with antibodies against B220 and CD43. Flow cytometry enumerations were performed within lymphocyte scatter gates. Percentages of cells in the marked gates are indicated. (*E*) Histological analysis of adult *Cxcr7*$^{-/-}$ spleen. Sections were stained with antibodies against B220 (green) and CD1d (red). The splenic MZ is indicated (bar).

to findings reported for *Cxcl12*$^{-/-}$ or *Cxcr4*$^{-/-}$ mice (3). Analysis of spleens of two surviving adult *Cxcr7*$^{-/-}$ mice revealed a modest but consistent reduction in the MZ B cell population that nonetheless localized normally to the splenic MZ (Fig. 1*E*). This was confirmed in *Mx1-Cre*/+*Cxcr7*$^{lox/lox}$ mice, in which CXCR7 deletion is induced after polyI:C injection (19) (not shown). Moreover, in contrast to *Cxcl12*$^{-/-}$ or *Cxcr4*$^{-/-}$ mice, neural development of *Cxcr7*$^{-/-}$ mice was indistinguishable from that of WT mice (SI Fig. 8), in keeping with normal levels of *Cxcr4* expression in the CNS (SI Fig. 9), as well as gastrointestinal vascularization (SI Fig. 10). Therefore, CXCR7 does not mediate CXCL12-driven hematopoietic functions and appears to be essential neither for MZ B cell localization to the splenic MZ nor for CXCL12-mediated functions in neural and gastrointestinal vasculature development.

Abnormal Heart Valve Development in *Cxcr7*$^{-/-}$ Mice. Sudden death of one of the five surviving *Cxcr7*$^{-/-}$ adult mice revealed the presence of a severely calcified aortic valve (not shown). In another two surviving *Cxcr7*$^{-/-}$ adults, aortic valve leaflets were thickened and in one of them fused, with clear evidence of chondrification (Fig. 2 *A–F*). Similar phenotypes were also observed in 10% of adult *Cxcr7*$^{+/-}$ mice. In 80% of *Cxcr7*$^{-/-}$ neonates, the heart was abnormal with dilatation of the right ventricle (Fig. 2 *G* and *H*). Submembranous ventricular septal defects were detected in 50% of *Cxcr7*$^{-/-}$ mice, with an associated overriding aorta in some cases (SI Table 1 and Fig. 2 *I* and *J*). Atrial septal defects were also observed (SI Table 1). All *Cxcr7*$^{-/-}$ mice showed a defect in at least one of the semilunar valves (SLVs) (SI Table 1 and Fig. 2 *K–V*). More than 90% of *Cxcr7*$^{-/-}$ neonates had an anomalous pulmonary valve, most of the time tricuspid with obviously thickened leaflets (77% of cases; compare Fig. 2 *O* and *P*), sometimes bicuspid (10%, Fig. 2*Q*), and very occasionally obstructed by an overgrown leaflet (5%, Fig. 2*R*). A similar range of anomalies was detected in the aortic valve of 70% of *Cxcr7*$^{-/-}$ neonates (Fig. 2 *K–N*, SI Table 1). Histological analysis confirmed these findings (Fig. 2 *S–V*). Embryonic hearts did not show any difference in outflow tract and atrioventricular cushion structure until E17.5 (not shown), suggesting that the early steps of cushion formation were not affected. We never observed anomalies of septation between the aorta and pulmonary artery. In addition, the tricuspid and mitral valves appeared normal at all stages examined (SI Fig. 11 *A–H*).

***Cxcr7* Is Expressed in Cardiac Microvessels, and Specific *Cxcr7* Deletion in the Endothelium Recapitulates the Heart Defects Seen in *Cxcr7*$^{-/-}$ Mice.** Examination of *Cxcr7* expression during embryogenesis, using *in situ* hybridization (ISH), revealed *Cxcr7* transcripts in the endothelial layer of the forming heart from E9.5 (Fig. 3 *A* and *C*). At this stage, strong expression was also detected in the neural tube, the brain, and the septum transversum (not shown). At E12.5, *Cxcr7* expression was detected in the mesenchyme of the forming valves as well as in numerous microvessels in the myocardium (Fig. 3*E*). From E14.5 onward, expression could no longer be detected in the mesenchyme, and *Cxcr7* was transcribed mainly in the microvasculature associated with myocardium, valves, and great vessels (Fig. 3*H*). *Cxcr4* transcripts were specific to the endothelium of valve-forming regions and their corresponding mesenchyme at E10.5, significantly overlapping with that of *Cxcr7* in the outflow tract (Fig. 3 *B* and *D*). From E12.5, *Cxcr4* and *Cxcr7* were expressed in a very similar manner, with diminishing levels of transcripts in valve mesenchyme and strong expression in the microvasculature of the developing valves and myocardium (Fig. 3 *E*, *F*, *H*, and *I*). At the same stages, expression of *Cxcl12* was undetectable in valve primordia but abundant in the aorta walls and myocardium-associated microvasculature (Fig. 3 *G* and *J*). Expression of *Cxcr4* and *Cxcl12* in embryos at various stages was comparable between WT and *Cxcr7*$^{-/-}$ mice (data not shown). In conclusion, in the developing heart, *Cxcl12*, *Cxcr4*, and *Cxcr7* are expressed in the myocardial microvasculature, whereas only *Cxcr4* and *Cxcr7* were transcribed in the valve mesenchyme and associated microvasculature.

We specifically deleted the *Cxcr7* gene in endothelium using *Tie2-Cre* transgenic mice (20). Forty percent of *Tie2-Cre*/+ *Cxcr7*$^{lox/lox}$ neonates were born with defects in SLVs, similar to those observed in *Cxcr7*$^{-/-}$ mice (SI Table 1), thus confirming the endothelial origin of the SLV defect in *Cxcr7*$^{-/-}$ mice. The lower penetration observed in *Tie2-Cre*/+ *Cxcr7*$^{lox/lox}$ mice was likely due to incomplete deletion of *Cxcr7* by the *Tie2-Cre* transgene, and indeed residual expression of *Cxcr7* was detected in hearts of nonaffected *Tie2-Cre*/+ *Cxcr7*$^{lox/lox}$ pups by ISH (not shown).

Impaired Expression of the Angiogenic Factor *Hbegf* and the Vasculo-Protector *Adrenomedullin* in *Cxcr7*$^{-/-}$ Cardiac Valves. We performed Affymetrix gene profiling on WT and *Cxcr7*$^{-/-}$ neonatal SLV leaflets. The abnormal remodeling of *Cxcr7*$^{-/-}$ heart valves shown in Fig. 2 *K–V* was highlighted by alterations of expression of extracellular matrix components such as *Eln*, *Fmod*, *Col9a1*, *Col14a1*, and *Mmp14* (Fig. 4*A*). Recently, SLV dysmorphogenesis has been associated with mutations of *Notch1* (21), *eNos* (*Nos3*) (22), *Phospholipase Cε1* (*Plce1*) (23), *Nfatc1* (24), *Fibrillin1* (*Fbn1*) (25), *Adam19* (26), *Smad6* (27), and various members of the HB-EGF pathway (*Hbegf*, *Egfr*, *Adam17*, and *Ptpn11*) (28–32). Transcript levels of most of these genes, assessed by ISH

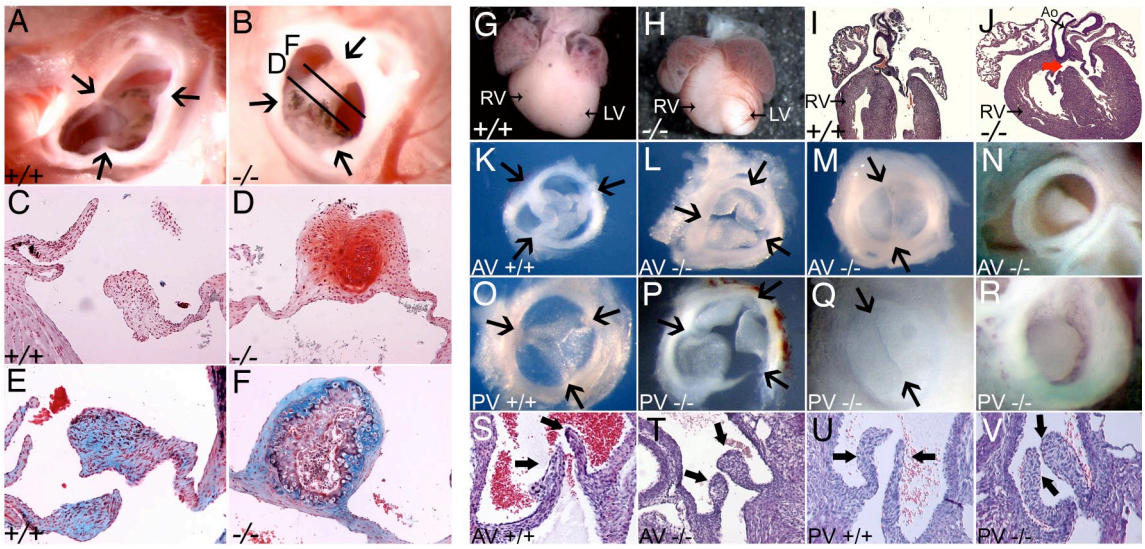

Fig. 2. SLV dysmorphogenesis in *Cxcr7*$^{-/-}$ mice. Adult aortic valve from control; (*A*, *C*, and *E*) and *Cxcr7*$^{-/-}$ (*B*, *D*, and *F*) mice. Arrows indicate leaflet boundaries. (*A* and *B*) Supravalvular view. Planes of sections shown in *D* and *F* are indicated. (*C–F*) Sections through the valves presented in *A* and *B*. (*C* and *D*) Safranin O staining; red indicates proteoglycans and glucosaminoglycans. (*E* and *F*) Movat pentachrome staining; blue indicates proteoglycans. Neonatal phenotype: (*G* and *H*) Dissected control and *Cxcr7*$^{-/-}$ (−/−) hearts. Right ventricle (RV) is often dilated in *Cxcr7*$^{-/-}$ mice. (*I* and *J*) Haematoxylin/eosin-counterstained sections of control and *Cxcr7*$^{-/-}$ hearts. Membranous ventricular septal defects (VSD, red arrow) and sometimes overriding aorta can be seen in mutants. Dissected aortic (*K–N*) and Pulmonary (*O–R*) valves from control and *Cxcr7*$^{-/-}$ neonates. Arrows indicate leaflet boundaries. Control aortic (*K*) and pulmonary (*O*) valves. (*L–M*, *P–R*): Phenotypical alterations in mutant valves ranging from thickening, with occasional fusion of valve leaflets (*L* and *P*), to formation of a bicuspid valve (*M* and *Q*), to obstruction of the valve by an overgrown leaflet (*N* and *R*). (*S–V*) Sections through the neonatal aortic (*S* and *T*) or pulmonary (*U* and *V*) valves of control (*S* and *U*) or *Cxcr7*$^{-/-}$ (*T* and *V*) mice. Black arrows point to valve leaflets. AV, aortic valve; PV, pulmonary valve; LV, left ventricle; Ao, aorta.

(SI Table 2) and/or on gene chips (Fig. 4*B*) were similar in WT and *Cxcr7*$^{-/-}$ valves at birth and during embryogenesis. However, expression of *Hbegf* was down-regulated 2- to 4-fold in neonatal *Cxcr7*$^{-/-}$ SLVs, which we confirmed by quantitative PCR (Fig. 4*D*). Other organs, including the myocardium, retained normal levels of expression (Fig. 4*D*). Valve thickening in *Hbegf*$^{-/-}$ mice is associated with increased bone morphogenetic protein signaling and proliferation in valve cells at midgestation (30). We observed similar effects in *Cxcr7*$^{-/-}$ heart valves (Fig. 4 *E–H*). Gene profiling of *Cxcr7*$^{-/-}$ SLV leaflets also revealed a dramatic reduction in expression of *Adrenomedullin* (*Adm*) compared with controls (Fig. 4*C*). In addition, expression of some genes linked to the function of Adm, such as complement factor H (*Cfh*), von Willebrand factor (*Vwf*), and *Col9a1* (33), were also significantly altered in *Cxcr7*$^{-/-}$ SLVs (Fig. 4*C*). *Adm* expression was unaffected in other neonatal *Cxcr7*$^{-/-}$ tissues tested (Fig. 4*D*). Therefore, down-regulation of *Adm*, like *Hbegf*, appeared not to be a general defect but rather restricted to SLV leaflets. Valve microvessels cells could not be isolated from leaflets in numbers high enough for culture. This precluded any attempt to demonstrate *ex vivo* modulation of *Hbegf* and *Adm* expression in response to CXCL12 or CXCL11. We have tested other systems of cultured endothelial cells and could not show modulation of these two genes in response to CXCL12 or CXCL11 (data not shown). This suggests either that modulation of *Hbegf* and *Adm* expression is either an indirect consequence of *Cxcr7* deletion, or that CXCR7-dependent expression of these genes is restricted to the developing valve leaflets.

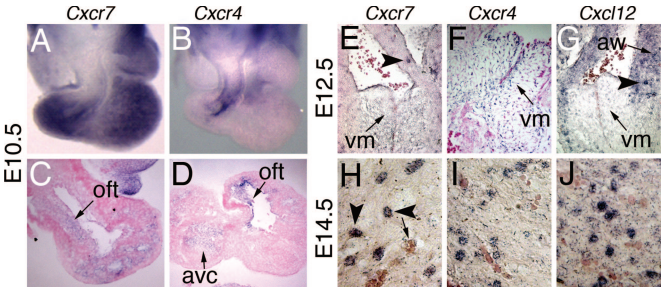

Fig. 3. Expression of *Cxcr7*, *Cxcr4*, and *Cxcl12* during heart embryogenesis. ISHs with probes specific to *Cxcr7* (*A*, *C*, *E*, and *H*), *Cxcr4* (*B*, *D*, *F*, and *I*), and *Cxcl12* (*G* and *J*). (*A* and *B*) Dissected E10.5 hearts. (*C* and *D*) Sections through endothelial cushions of *A* and *B*. (*E–G*) Sections throughout SLVs of E12.5 embryos. (*H–J*) Sections through myocardium of E14.5 embryos. Avc, atrioventricular canal; Oft; the ouflow tract points; Vm, valve mesenchyme. Arrowheads point to microvasculature; the arrow in *H* points to unstained coronary vessel.

CXCL12 and CXCL11 Are the Only Two Chemokine Ligands of CXCR7. SLVs develop normally in *Cxcl12*$^{-/-}$ mice (4), suggesting that a ligand distinct from CXCL12 may be involved in CXCR7 function in valve morphogenesis (18). We tested the ability of a range of chemokines to compete with ^{125}I-CXCL12 binding to human CXCR7 transfectants (SI Fig. 12*A*). Only CXCL12 (SDF-1) and CXCL11 (ITAC) could displace ^{125}I-CXCL12 binding, and CXCL11 was not as efficient as cold CXCL12 (SI Fig. 12*B*), similar to recently published findings (8, 9). However, alignment of the *Cxcl11* sequence from various mouse strains showed that C57BL/6, the genetic background of *Cxcr7*$^{-/-}$ mice are natural null mutants for *Cxcl11* (SI Fig. 12*C*), because a 2-bp insertion soon after the start codon of the C57BL/6 sequence creates a frameshift resulting in a premature stop codon. Because C57BL/6 mice develop normally in the absence of a functional copy of *Cxcl11*, CXCL11/CXCR7 interaction is unlikely to play a nonredundant role in SLV formation.

CXCR7 and CXCR4 Form Heterodimers, Potentiating Signaling in Response to CXCL12. We and others (9) have failed to detect calcium flux or migratory behavior of CXCR7-expressing cells after stimulation with CXCL12 or CXCL11. Moreover, the DRYLAIV motif conserved in most chemokine receptors and

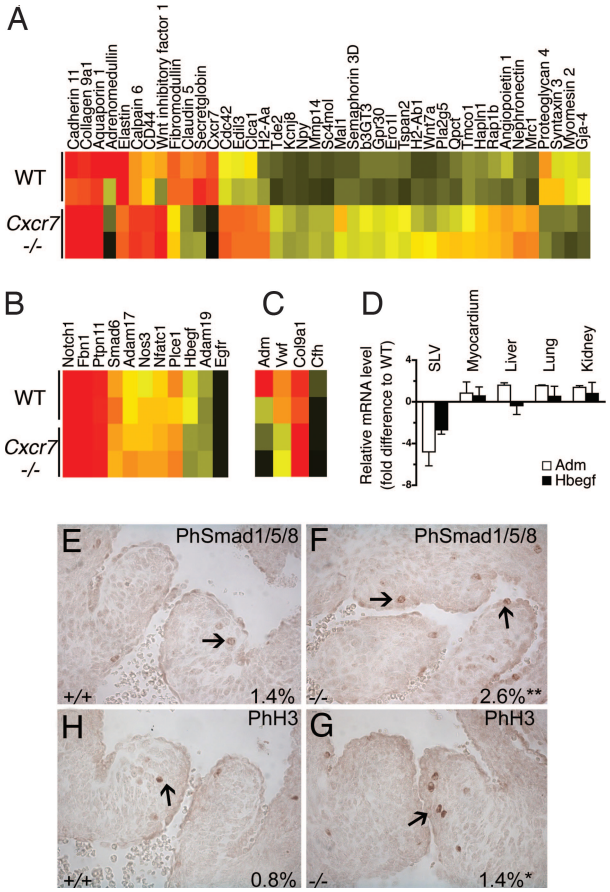

Fig. 4. Gene profiling of neonatal *Cxcr7*$^{-/-}$ SLVs. Heat maps of ECM and adhesion genes differentially expressed in WT and *Cxcr7*$^{-/-}$ dissected SLV leaflets (*A*), genes associated with SLV defects (*B*), and genes linked to Adm function (*C*). Signal intensity is color-coded (*A–C*). (*D*) qRT-PCR analysis of *Hbegf* and *Adm* expression in various control and *Cxcr7*$^{-/-}$ neonatal organs. Values ± SEM. (*E–H*) PhosphoSmad1/5/8 or phosphohistone H3 immunohistological staining on sections of E14.5 control (+/+) and *Cxcr7*$^{-/-}$ (−/−) SLVs. Percentage of positive nuclei in SLVs per staining and genotype are indicated. *, $P < 0.01$; **, $P < 0.001$.

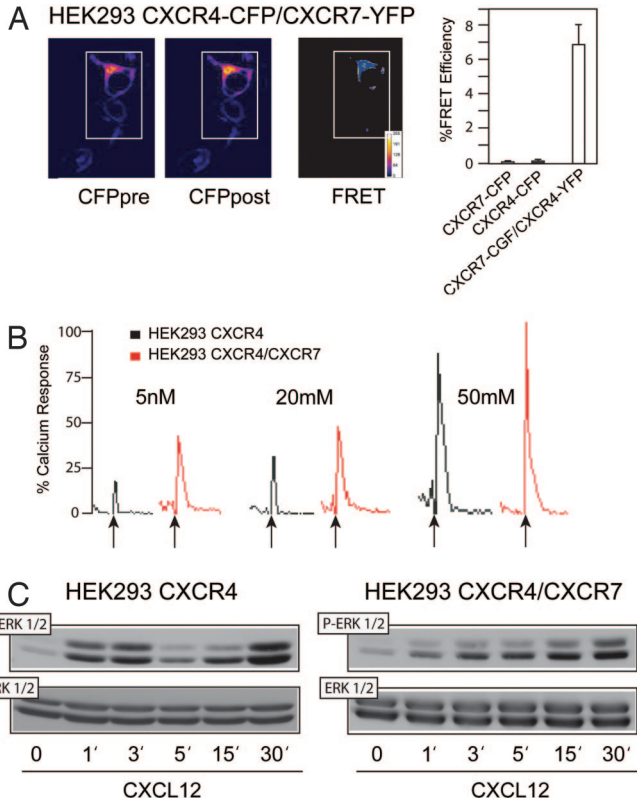

Fig. 5. CXCR4 and CXCR7 form functional heterodimers. (*A*) FRET measurements in unstimulated HEK293 cells transiently transfected with CXCR4-CFP and CXCR7-YFP. CFP emission before (CFPpre) and after YFP bleaching (CFPpost) and a false-color merged image (FRET) are shown. Data are expressed as percentage of FRET efficiency ± SD. (*B*) Representative Ca^{2+} flux triggered by CXCL12 on HEK293 cells expressing both CXCR7 and CXCR4 or only-CXCR4. Results are expressed as a percentage of the maximum chemokine-induced Ca^{2+} response. (*C*) Anti-phospho-ERK immunoblot after CXCL12 stimulation of HEK293 or CXCR7-transfected HEK293. Protein loading was controlled with an anti-ERK antibody.

considered necessary for G protein coupling and calcium signaling (34) is altered to DRYLSIT in CXCR7. Thus CXCR7 may not function as a classical chemokine receptor but could behave as a decoy or chemokine-transporting receptor, similar to other endothelial-expressed receptors such as D6, CCX-CKR, and DARC (34). An alternative explanation is that CXCR7 may not function alone but may modulate CXCR4 functions via formation of heterodimeric complexes as shown for other chemokine receptors (35–37), although the importance of this phenomenon *in vivo* is not known. We tested this hypothesis using FRET, a technique that allows temporal and spatial resolution of heterodimeric complexes.

HEK293 cells transiently transfected with CXCR4–cyan fluorescent protein (CFP) and CXCR7–yellow fluorescent protein (YFP) were used for FRET analysis. Preformed dimers of CXCR4 and CXCR7 were detected at the cell membrane in the absence of ligand, with evidence also of intracellular heterodimer pools (Fig. 5*A*). Immunoprecipitation experiments using HEK293 cells (which endogenously express CXCR4), CXCR7-stably transfected HEK293 cells, or IM-9 cells that naturally express CXCR4 and low levels of CXCR7 (SI Fig. 13 *A–D*), in the presence or absence of CXCL12, confirmed the presence of CXCR7/CXCR4 heterodimers in the absence of ligand in both cell lines (SI Fig. 13 *A* and *D*).

Chemokine receptor heterodimerization increases the sensitivity and dynamic range of the chemokine response (35). We evaluated CXCL12-induced Ca^{2+} flux in both HEK293 and CXCR7-stably transfected HEK293 cells. Addition of CXCL12 induced a stronger Ca^{2+} flux in cells coexpressing CXCR4 and CXCR7 than in control (CXCR4 only) cells (Fig. 5*B*). Chemokines trigger MAPK activation (38, 39), and heterodimers can activate signaling pathways that differ from those activated by homodimers (35). We evaluated whether coexpression of CXCR7 could affect CXCL12-induced ERK1/2 phosphorylation via CXCR4 using stably transfected HEK293 cells. Whereas a biphasic activation of ERK was detected in cells that express CXCR4 only, with peaks at 3 and 30 min, in cells coexpressing CXCR4 and CXCR7, CXCL12 induced a delayed peak of ERK activation without the initial spike (Fig. 5*C* and SI Fig. 13*E*). In conclusion, CXCR4/CXCR7 form heterodimers, and coexpression of these two receptors induces a stronger Ca^{2+} flux than CXCR4 alone and modulates downstream signaling through ERK1/2.

Discussion

CXCR7 is a highly conserved chemokine receptor that binds with high affinity to the chemokine CXCL12. Similar to the other CXCL12 receptor CXCR4, CXCR7 is widely expressed and plays a role in fetal development. *Cxcr7*$^{-/-}$ mice showed atrial septal defects and submembranous ventricular septal

defects as well as impaired SLV remodeling but to date no obvious immune or brain phenotype.

Endothelial-specific inactivation using *Tie2-Cre* mice recapitulated *Cxcr7*$^{-/-}$ mice phenotype, supporting a predominant role for CXCR7 in endothelial biology.

We observed a dramatic phenotype in *Cxcr7*$^{-/-}$ mice, despite this receptor showing no apparent signaling to its ligand CXCL12. A possible explanation is that CXCR7 forms heterodimers with CXCR4 and modulates CXCR4 signaling to CXCL12. In the heart, *Cxcr7* expression only significantly overlaps with *Cxcr4* expression in the valve-forming regions, the outflow tract mesenchyme in particular, and later in the microvasculature. Therefore, heterodimerization of the corresponding proteins at these sites could be required for proper valve morphogenesis. Recent findings indicate that many G protein-coupled seven-transmembrane receptors, including chemokine receptors, exist as homo- and heterodimers, and that these conformations may be important in aspects of receptor biology that range from ontogeny to regulation of pharmacological and signaling properties (37, 40, 41). At the immunological synapse, CXCR4/CCR5 heterodimers recruit the $G\alpha_q$ subunit (rather than the $G\alpha_i$) and induce costimulatory signals to T cells (36). Indeed, heterodimerization and associated effects on signaling may be one mechanism that accounts for the widespread expression of nonsignaling chemokine receptors in endothelium (34). Nevertheless, the significance of chemokine receptor heterodimerization *in vivo* remains uncertain. The phenotypic differences described for *Cxcr7*$^{-/-}$ (reported here) and *Cxcr4*$^{-/-}$ mice (3, 5–7), and recent work examining the role of these receptors in zebrafish development (42, 43), support an alternative hypothesis, that CXCR7 and CXCR4 can have separate biological roles.

A recent study showed that CXCR7 facilitated angiogenesis, and blockade of CXCR7 inhibited tumor growth in mouse models (9). We did not observe any gross difference in the density of the microvasculature in *Cxcr7*$^{-/-}$ mice; however, deficiency of *Cxcr7* correlated with down-regulation of at least two endothelial-expressed angiogenic genes in neonatal valves, *Hbegf* and *Adm*. Mutations in components of the HB-EGF pathway lead to increased bone morphogenetic protein signaling and proliferation, associated with valve thickening (27, 30, 32, 44). Similar alterations were observed in *Cxcr7*$^{-/-}$ SLVs, suggesting that the valve phenotype of *Cxcr7*$^{-/-}$ mice stems in part from partial down-regulation of *Hbegf*. By ISH, expression patterns of *Hbegf* and *Cxcr7* were very similar at midgestation, and conditional inactivation of *Hbegf* using *Tie2Cre* recapitulated the valve defects found in embryos homozygous for the full null allele (31). However, more *Hbegf*$^{-/-}$ mice survive (40%) than *Cxcr7*$^{-/-}$ mice (30), implying other alterations contributing to the phenotype in *Cxcr7*$^{-/-}$ mice. We observed a marked down-regulation of *Adm* at birth, a known vasculoprotector critical for embryonic development (45). *Adm* expression was unaffected in all other tissues tested, and it is unclear whether its down-regulation in SLVs was a cause or a consequence of the observed heart valve phenotype. Combined down-regulation of both *Hbegf* and *Adm* might trigger a severe impairment of SLV function, and potentially the early lethality observed *Cxcr7*$^{-/-}$ mice.

SLVs develop normally in *Cxcl12*$^{-/-}$ mice (4), suggesting that a ligand distinct from CXCL12 may be involved in CXCR7 function in valve morphogenesis. However, because *Cxcl12*$^{-/-}$ mice were generated on a mixed 129xC57BL/6 background and express CXCL11, we cannot exclude a compensatory signaling role for CXCL11 via CXCR7 in these mice. Furthermore, because C57BL/6 mice develop normally in the absence of a functional copy of *Cxcl11*, CXCL11/CXCR7 interaction is unlikely to play a nonredundant role in SLV formation. Therefore, although CXCL12 and CXCL11 may normally be functionally redundant, there may also be an as-yet-unidentified ligand for CXCR7 involved in valve morphogenesis.

The phenotypes of mice lacking *Cxcl12*, *Cxcr4*, or *Cxcr7* highlight the essential role of certain chemokines and receptors in embryonic development. It is conceivable that the original evolutionary function of chemokine receptors was to serve as guidance molecules during embryonic or fetal development, and CXCL12 binding to CXCR4 has a clear role in such processes (1). The immune system may have adopted, duplicated, and refined certain receptors specifically for immune cell migration. Our results reveal distinct roles for the two CXCL12 receptors, CXCR7 and CXCR4. CXCR7 plays an important role in cardiac development and further studies are needed to determine the precise connection between this role and its role in tumor angiogenesis (9). Regardless, study of the role of CXCR7 through gene deletion has provided insight into heart valve morphogenesis, which ultimately may have relevance for the identification of additional factors that contribute to heart valve defects in humans.

Materials and Methods

Generation of *Cxcr7*$^{lox/+}$ Mice. *Cxcr7*$^{lox/+}$ mice were generated at Ozgene (Bentley DC, Australia). Briefly, LoxP sites were inserted around exon 2, which encodes CXCR7, in C57BL/6 *Cxcr7* genomic DNA. Bruce 4 C57BL/6 ES cells were electroporated. Chimeric males generated with *Cxcr7*$^{lox/+}$ ES cells were mated to C57BL/6J females to obtain *Cxcr7*$^{lox/+}$ mice. *Cxcr7*$^{lox/+}$ mice were crossed to C57BL/6 *CMV-Cre* (46) or C57BL/6 *Tie2-Cre*/+ transgenic mice (20) to generate germ-line or endothelial-specific deletion of *Cxcr7* (SI Fig. 6). All experimental procedures involving mice were carried out according to protocols approved by the Garvan Institute /St. Vincent's Hospital Animal Ethics Committee and the Animal Resources Center/Ozgene Animal Ethics Committee.

Immunohistochemistry and Cytochemistry. Immunohistochemistry and cytochemistry were performed after fixation in 4% paraformaldehyde and wax embedding. Anti-PhosphoSmad1/5/8 (9511S; Cell Signaling Technology, Beverly, MA) and Phospho-Histone H3 (06-570; Upstate Biotechnology, Lake Placid, NY) were applied after an antigen retrieval step in citrate buffer for 8 min at subboiling temperature. At least three sections across each SLV of two controls and two mutants were counted (>2,000 cells per genotype). Statistical analysis was done using a χ^2 test. Cytochemistry for chloroacetyl esterase was done on paraffin-embedded sections of femurs from E17.5 embryos using an esterase activity staining kit (Sigma–Aldrich, St. Louis, MO), following the manufacturer's protocol. Ten-micrometer sections were stained with a Russell-Movat pentachrome stain kit (American Master Tech Scientific, Lodi, CA) following the manufacturer's protocol. Other sections were stained with Safranin O.

RNA Extraction, GeneChip Hybridization, and Gene Profile Analysis. Affymetrix 430 2.0 GeneChips were hybridized with cRNA synthesized from RNA from neonate SLVs dissected under the microscope. Two different pools of WT and mutant SLV RNAs were used in independent hybridizations. cRNA was prepared, and GeneChips were hybridized and scanned as previously described (16). Analysis of gene profiles is described in more detail in *SI Text*.

qRT-PCR. cDNA was synthesized from 100 ng of total RNA using Reverse-IT RTase Blend Kit (Abgene, Surrey, U.K.), following the manufacturer's indications. Quantitation was performed on at least three independent WT and *Cxcr7*$^{-/-}$ samples for each tissue analyzed, and experiments were carried out in triplicate. β-actin was used to standardize the total amount of cDNA. Primer sequences can be found in SI Table 3.

ISH. ISH was performed by using a conventional protocol (see *SI Text*). Probe templates were amplified by using primers described in SI Table 3 and verified by sequencing.

FRET. FRET was measured by photobleaching of HEK293 cells (American Type Culture Collection TIB202) transiently transfected at a 1:1 ratio with CXCR4-CFP and CXCR7-YFP and cultured in coverslip chambers (Nunc, Rochester, NY) for 48 h. Identical results were obtained with CXCR7-CFP and CXCR4-YFP. Cells were imaged by using a laser-scanning confocal microscope (Olympus, Tokyo, Japan; IX81). HEK293 cells transfected with CXCR4-CFP and CXCR7-CFP were used as negative controls. Data are reported as mean ± SD. Statistical significance was tested by using the unpaired Student's *t* test. Detailed description of a typical FRET experiment is available in *SI Text*.

Western Blot. A 20 nM concentration of CXCL12-stimulated HEK293 cells or CXCR7 stably transfected HEK293 cells or IM-9 cells (2×10^7) were lysed in 20 mM triethanolamine (pH 8.0), 300 mM NaCl, 2 mM EDTA, 20% glycerol, 2% digitonin, 10 mM sodium orthovanadate, 10 μg/ml leupeptin, 10 μg/ml aprotinin for 30 min at 4°C and then centrifuged (15,000 × *g*, 15 min, 4°C) and processed for Western blot with anti-phospho-ERK1/2 (Santa Cruz Biotechnology, Santa Cruz, CA).

Calcium Determination. Untransfected or CXCR7-stably transfected HEK293 cells (2.5×10^6 cells/ml) were resuspended in RPMI medium 1640 containing 10% FCS and 10 mM Hepes and incubated with Fluo-3 (Calbiochem, La Jolla, CA). Cells were washed, resuspended in RPMI containing 2 mM $CaCl_2$, and maintained at 4°C before adding CXCL12. Calcium flux was measured at 525 nm in an EPICS XL flow cytometer (Coulter, Hialeah, FL).

We thank O. Prall, M. Costa, M. Furtado, S. Liu, J. Zaunders, and R. Bouveret for comments on the manuscript and R. G. Graham for helpful discussions. This work is supported by the National Health and Medical Research Council (Australia), the Wellcome Trust (U.K.), and the NSW Cancer Research Institute.

1. Doitsidou M, Reichman-Fried M, Stebler J, Koprunner M, Dorries J, Meyer D, Esguerra CV, Leung T, Raz E (2002) *Cell* 111:647–659.
2. Mackay CR (2001) *Nat Immunol* 2:95–101.
3. Zou YR, Kottmann AH, Kuroda M, Taniuchi I, Littman DR (1998) *Nature* 393:595–599.
4. Nagasawa T, Hirota S, Tachibana K, Takakura N, Nishikawa S, Kitamura Y, Yoshida N, Kikutani H, Kishimoto T (1996) *Nature* 382:635–638.
5. Ma Q, Jones D, Borghesani PR, Segal RA, Nagasawa T, Kishimoto T, Bronson RT, Springer TA (1998) *Proc Natl Acad Sci USA* 95:9448–9453.
6. Bagri A, Gurney T, He X, Zou YR, Littman DR, Tessier-Lavigne M, Pleasure SJ (2002) *Development (Cambridge, UK)* 129:4249–4260.
7. Lu M, Grove EA, Miller RJ (2002) *Proc Natl Acad Sci USA* 99:7090–7095.
8. Balabanian K, Lagane B, Infantino S, Chow KY, Harriague J, Moepps B, Arenzana-Seisdedos F, Thelen M, Bachelerie F (2005) *J Biol Chem* 280:35760–35766.
9. Burns JM, Summers BC, Wang Y, Melikian A, Berahovich R, Miao Z, Penfold ME, Sunshine MJ, Littman DR, Kuo CJ, *et al.* (2006) *J Exp Med* 203:2201–2213.
10. Heesen M, Berman MA, Charest A, Housman D, Gerard C, Dorf ME (1998) *Immunogenetics* 47:364–370.
11. Broberg K, Zhang M, Strombeck B, Isaksson M, Nilsson M, Mertens F, Mandahl N, Panagopoulos I (2002) *Int J Oncol* 21:321–326.
12. Burger JA, Kipps TJ (2006) *Blood* 107:1761–1767.
13. Busillo JM, Benovic JL (2006) *Biochim Biophys Acta* 1768:952–963.
14. Salcedo R, Oppenheim JJ (2003) *Microcirculation* 10:359–370.
15. Su AI, Cooke MP, Ching KA, Hakak Y, Walker JR, Wiltshire T, Orth AP, Vega RG, Sapinoso LM, Moqrich A, *et al.* (2002) *Proc Natl Acad Sci USA* 99:4465–4470.
16. Chtanova T, Newton R, Liu SM, Weininger L, Young TR, Silva DG, Bertoni F, Rinaldi A, Chappaz S, Sallusto F, *et al.* (2005) *J Immunol* 175:7837–7847.
17. Liu SM, Xavier R, Good KL, Chtanova T, Newton R, Sisavanh M, Zimmer S, Deng C, Silva DG, Frost MJ, *et al.* (2006) *J Allergy Clin Immunol* 118:496–503.
18. Infantino S, Moepps B, Thelen M (2006) *J Immunol* 176:2197–2207.
19. Kuhn R, Schwenk F, Aguet M, Rajewsky K (1995) *Science* 269:1427–1429.
20. Koni PA, Joshi SK, Temann UA, Olson D, Burkly L, Flavell RA (2001) *J Exp Med* 193:741–754.
21. Garg V, Muth AN, Ransom JF, Schluterman MK, Barnes R, King IN, Grossfeld PD, Srivastava D (2005) *Nature* 437:270–274.
22. Lee TC, Zhao YD, Courtman DW, Stewart DJ (2000) *Circulation* 101:2345–2348.
23. Tadano M, Edamatsu H, Minamisawa S, Yokoyama U, Ishikawa Y, Suzuki N, Saito H, Wu D, Masago-Toda M, Yamawaki-Kataoka Y, *et al.* (2005) *Mol Cell Biol* 25:2191–2199.
24. de la Pompa JL, Timmerman LA, Takimoto H, Yoshida H, Elia AJ, Samper E, Potter J, Wakeham A, Marengere L, Langille BL, *et al.* (1998) *Nature* 392:182–186.
25. Pyeritz RE (2000) *Annu Rev Med* 51:481–510.
26. Zhou HM, Weskamp G, Chesneau V, Sahin U, Vortkamp A, Horiuchi K, Chiusaroli R, Hahn R, Wilkes D, Fisher P, *et al.* (2004) *Mol Cell Biol* 24:96–104.
27. Galvin KM, Donovan MJ, Lynch CA, Meyer RI, Paul RJ, Lorenz JN, Fairchild-Huntress V, Dixon KL, Dunmore JH, Gimbrone MA, Jr, *et al.* (2000) *Nat Genet* 24:171–174.
28. Iwamoto R, Yamazaki S, Asakura M, Takashima S, Hasuwa H, Miyado K, Adachi S, Kitakaze M, Hashimoto K, Raab G, *et al.* (2003) *Proc Natl Acad Sci USA* 100:3221–3226.
29. Iwamoto R, Mekada E (2006) *Cell Struct Funct* 31:1–14.
30. Jackson LF, Qiu TH, Sunnarborg SW, Chang A, Zhang C, Patterson C, Lee DC (2003) *EMBO J* 22:2704–2716.
31. Nanba D, Kinugasa Y, Morimoto C, Koizumi M, Yamamura H, Takahashi K, Takakura N, Mekada E, Hashimoto K, Higashiyama S (2006) *Biochem Biophys Res Commun* 350:315–321.
32. Chen B, Bronson RT, Klaman LD, Hampton TG, Wang JF, Green PJ, Magnuson T, Douglas PS, Morgan JP, Neel BG (2000) *Nat Genet* 24:296–299.
33. Garcia-Unzueta MT, Berrazueta JR, Pesquera C, Obaya S, Fernandez MD, Sedano C, Amado JA (2005) *J Diabetes Compl* 19:147–154.
34. Haraldsen G, Rot A (2006) *Eur J Immunol* 36:1659–1661.
35. Mellado M, Rodriguez-Frade JM, Vila-Coro AJ, Fernandez S, Martin de Ana A, Jones DR, Toran JL, Martinez AC (2001) *EMBO J* 20:2497–2507.
36. Molon B, Gri G, Bettella M, Gomez-Mouton C, Lanzavecchia A, Martinez AC, Manes S, Viola A (2005) *Nat Immunol* 6:465–471.
37. Percheranciер Y, Berchiche YA, Slight I, Volkmer-Engert R, Tamamura H, Fujii N, Bouvier M, Heveker N (2005) *J Biol Chem* 280:9895–9903.
38. Ganju RK, Brubaker SA, Meyer J, Dutt P, Yang Y, Qin S, Newman W, Groopman JE (1998) *J Biol Chem* 273:23169–23175.
39. Thelen M (2001) *Nat Immunol* 2:129–134.
40. Babcock GJ, Farzan M, Sodroski J (2003) *J Biol Chem* 278:3378–3385.
41. Terrillon S, Bouvier M (2004) *EMBO Rep* 5:30–34.
42. Valentin G, Haas P, Gilmour D (2007) *Curr Biol* 17:1026–1031.
43. Dambly-Chaudiere C, Cubedo N, Ghysen A (2007) *BMC Dev Biol* 7:23–37.
44. Choi M, Stottmann RW, Yang YP, Meyers EN, Klingensmith J (2007) *Circ Res* 100:220–228.
45. Shimosawa T, Shibagaki Y, Ishibashi K, Kitamura K, Kangawa K, Kato S, Ando K, Fujita T (2002) *Circulation* 105:106–111.
46. Schwenk F, Baron U, Rajewsky K (1995) *Nucleic Acids Res* 23:5080–5081.